TRPM7 Provides an Ion Channel Mechanism for Cellular Entry of Trace Metal Ions

Mahealani K. Monteilh-Zoller,[1] Meredith C. Hermosura,[2] Monica J.S. Nadler,[3] Andrew M. Scharenberg,[4] Reinhold Penner,[1] and Andrea Fleig[1]

[1]Laboratory of Cell and Molecular Signaling, Center for Biomedical Research at The Queen's Medical Center and John A. Burns School of Medicine at the University of Hawaii, Honolulu, HI 96813

[2]Pacific Biomedical Research Center, University of Hawaii, Honolulu, HI 96822

[3]Department of Pathology, Beth Israel Deaconess Medical Center and Harvard Medical School, Boston, MA 02215

[4]Department of Pediatrics, University of Washington and Children's Hospital and Regional Medical Center, Seattle, WA 98195

ABSTRACT Trace metal ions such as Zn^{2+}, Fe^{2+}, Cu^{2+}, Mn^{2+}, and Co^{2+} are required cofactors for many essential cellular enzymes, yet little is known about the mechanisms through which they enter into cells. We have shown previously that the widely expressed ion channel TRPM7 (LTRPC7, ChaK1, TRP-PLIK) functions as a Ca^{2+}- and Mg^{2+}-permeable cation channel, whose activity is regulated by intracellular Mg^{2+} and Mg^{2+}·ATP and have designated native TRPM7-mediated currents as magnesium-nucleotide–regulated metal ion currents (MagNuM). Here we report that heterologously overexpressed TRPM7 in HEK-293 cells conducts a range of essential and toxic divalent metal ions with strong preference for Zn^{2+} and Ni^{2+}, which both permeate TRPM7 up to four times better than Ca^{2+}. Similarly, native MagNuM currents are also able to support Zn^{2+} entry. Furthermore, TRPM7 allows other essential metals such as Mn^{2+} and Co^{2+} to permeate, and permits significant entry of nonphysiologic or toxic metals such as Cd^{2+}, Ba^{2+}, and Sr^{2+}. Equimolar replacement studies substituting 10 mM Ca^{2+} with the respective divalent ions reveal a unique permeation profile for TRPM7 with a permeability sequence of $Zn^{2+} \approx Ni^{2+} >> Ba^{2+} > Co^{2+} > Mg^{2+} \geq Mn^{2+} \geq Sr^{2+} \geq Cd^{2+} \geq Ca^{2+}$, while trivalent ions such as La^{3+} and Gd^{3+} are not measurably permeable. With the exception of Mg^{2+}, which exerts strong negative feedback from the intracellular side of the pore, this sequence is faithfully maintained when isotonic solutions of these divalent cations are used. Fura-2 quenching experiments with Mn^{2+}, Co^{2+}, or Ni^{2+} suggest that these can be transported by TRPM7 in the presence of physiological levels of Ca^{2+} and Mg^{2+}, suggesting that TRPM7 represents a novel ion-channel mechanism for cellular metal ion entry into vertebrate cells.

KEY WORDS: zinc • magnesium • nucleotide • trp channel • cation channel

The Journal of General Physiology

INTRODUCTION

Aside from Ca^{2+}, whose fundamental role in countless cellular processes is well recognized (Berridge et al., 1999), and Mg^{2+}, which plays an important role in the modulation of ion channels, receptors, G proteins, and effector enzymes (Volpe and Vezu, 1993; Romani and Scarpa, 2000), the trace metal ions Fe^{2+}, Zn^{2+}, Cu^{2+}, Mn^{2+}, and Co^{2+} function as cofactors vital to the catalytic function of diverse types of enzymes involved in virtually every major cellular process (Hediger, 1997; Nelson, 1999). There exists a duality to metal ions: while undeniably crucial for cellular function, if they accumulate above trace levels, these ions are highly toxic. This is particularly true for zinc, which is one of the most abundant transition metals in the brain (Weiss et al., 2000; Koh, 2001). Excessive vesicular release of Zn^{2+} is thought to play a key role in neuronal cell death following ischemia (Choi and Koh, 1998). In addition to its acute neurotoxicity, zinc may contribute to the pathogenesis of chronic neurodegenerative conditions such as Alzheimer's disease, where it is found to accumulate in amyloid plaques (Lee et al., 2002).

Although considerable progress has been made toward understanding intracellular Ca^{2+} homeostasis, transport processes, and homeostatic mechanisms, the regulation of intracellular concentrations of other divalent metal ions remains poorly understood (Hediger, 1997; Nelson, 1999; Romani and Scarpa, 2000). So far, only few proteins with established roles in trace metal ion homeostasis are known: (a) the natural resistance–associated macrophage proteins (NRAMPs),* a family of proton-coupled divalent cation transporters of varying selectivity (Gunshin et al., 1997; Knopfel et al., 2000; Picard et al., 2000) and two more zinc-specific

Mahealani K. Monteilh-Zoller and Meredith C. Hermosura contributed equally to this work.

Address correspondence to Andrea Fleig, Center for Biomedical Research, The Queen's Medical Center University, Tower 8, 1301 Punchbowl Street, Honolulu, HI 96813. Fax: (808) 537-7899; E-mail: afleig@hawaii.edu

*Abbreviation used in this paper: NRAMP, natural resistance–associated macrophage protein.

J. Gen. Physiol. © The Rockefeller University Press • 0022-1295/2003/01/49/12 $8.00
Volume 121 January 2003 49–60
http://www.jgp.org/cgi/doi/10.1085/jgp.20028740

families of proteins, (b) the CDFs (cation diffusion facilitator), a family that includes the ZnT proteins, which are thought to be involved in zinc export and vesicular zinc transport (Cousins and McMahon, 2000; Harris, 2002), and the ZIPs (ZRT/IRT-related protein), a family that functions in zinc influx into cytoplasm (Gaither and Eide, 2000, 2001). However, there may be additional metal ion transport mechanisms available to cells.

Most divalent ions block ion fluxes through Ca^{2+}-permeable ion channels, with the exception of Sr^{2+} and Ba^{2+}, which are usually more permeable than Ca^{2+}. Nevertheless, various ion channels have been implicated in transporting divalent ions other than Ca^{2+}. For example, early reports on insect muscle membranes indicated permeation of Mn^{2+}, Cd^{2+}, Zn^{2+}, and beryllium (Be^{2+}) but not Co^{2+}, Ni^{2+}, or Mg^{2+} through calcium channels (Fukuda and Kawa, 1977). Later, endplate channels were shown to conduct trace metal ions including Co^{2+}, Ni^{2+}, Mg^{2+}, and Cd^{2+} (Adams et al., 1980). Furthermore, voltage-dependent and receptor-mediated influx pathways may allow some Mn^{2+} influx, which can be detected as fluorescence quench of fura-2 (Merritt et al., 1989; Jacob, 1990; Shibuya and Douglas, 1992; Fasolato et al., 1993a,b). The store-operated Ca^{2+} current I_{CRAC} has a very small Mn^{2+} permeability that can only be resolved electrophysiologically when using isotonic Mn^{2+} solutions (Hoth and Penner, 1993). Zn^{2+} permeation has been suggested for AMPA/kainate glutamate receptors (Weiss and Sensi, 2000) and voltage-dependent Ca^{2+} channels have been reported to carry small Zn^{2+} currents (Kerchner et al., 2000). Of the TRP-related ion channels, the vanilloid receptor VR1 has been suggested to have some limited Mg^{2+} permeability (Caterina et al., 1997) and the epithelial calcium channel ECaC1 (CaT2) has been reported to conduct Cd^{2+} (Peng et al., 2000). However, in most of these cases, the transport rates of divalent cations are a fraction of those achieved by the main permeant ion species and rarely large enough to be resolved by electrophysiological recordings.

TRPM7 (Nadler et al., 2001; Runnels et al., 2001), a widely expressed member of the TRPM family of ion channels (Harteneck et al., 2000; Montell et al., 2002) is a cation channel that is regulated by intracellular levels of Mg·ATP and is strongly activated when Mg·ATP falls below 1 mM, thereby producing a current that we have designated MagNuM for magnesium-nucleotide–regulated metal ion current (Nadler et al., 2001; Hermosura et al., 2002). Our initial analyses demonstrated that TRPM7 is similarly permeable to both of the dominant divalent cations Ca^{2+} and Mg^{2+}. We here report that TRPM7 is generally permeable to metal ions, exhibiting particularly high permeation of Zn^{2+}, but also permeating other essential divalent cations, including Mg^{2+}, Mn^{2+}, and Co^{2+} as well as the nonphysiological or toxic metal ions Ba^{2+}, Sr^{2+}, Ni^{2+}, and Cd^{2+}. These results suggest that TRPM7 acts as a ubiquitous metal ion influx pathway, the existence of which may have important implications for many physiological and pathological contexts.

MATERIALS AND METHODS

Cells

HEK-293 cells transfected with the FLAG-murineTRPM7/pCDNA4/TO construct were grown on glass coverslips with DMEM medium supplemented with 10% fetal bovine serum, with 10% FBS, blasticidin (5 μg/ml), and zeocin (0.4 mg/ml). TRPM7 expression was induced 1 d before use by adding 1 μg/ml tetracycline to the culture medium. Patch-clamp and fura-2 measurements were done 16–24 h postinduction. See Nadler et al. (2001).

Solutions

Cells grown on glass coverslips were transferred to the recording chamber and kept in a standard modified Ringer's solution of the following composition (in mM): NaCl 145, KCl 2.8, $CaCl_2$ 1, $MgCl_2$ 2, glucose 10, HEPES·NaOH 10, pH 7.2, with osmolarity typically ranging from 298–308 mOsm. In some experiments, $CaCl_2$ and $MgCl_2$ concentrations were adjusted as indicated in the text and figure legends. Intracellular pipette-filling solutions contained (in mM): Cs-glutamate 145, NaCl 8, $MgCl_2$ 1, Cs-BAPTA 10, HEPES·CsOH, pH 7.2 adjusted with CsOH. In some experiments, 10 mM Cs-BAPTA was replaced with 200 μM fura-2 and in others 3 mM Mg·ATP was added. For equimolar ion-substitution experiments, cells were bathed in a standard Ringer's solution containing 10 mM $CaCl_2$ and no added $MgCl_2$. This solution was temporarily replaced by an identical solution that contained 10 mM of the metal-chloride salt of the relevant test ion. Isotonic solutions were prepared from Cl^- salts of the relevant metal ions in distilled water at concentrations of 120 mM (osmolarities, 295–310 mOsm; pH, 5.1–5.5). The effects of pH were assessed in TRPM7-overexpressing cells by applying isotonic choline-Cl solutions (150 mM) without divalent ions and buffered to various pH values using 10 mM TRIS and HCl. These solutions completely inhibited inward currents through TRPM7 down to pH values of 4 (n = 5, unpublished data), indicating that the tested isotonic metal solutions (pH = 5.1–5.5) are not contaminated with proton currents. For the case of Zn^{2+}, we also prepared a choline-Cl–based solution that lacked any monovalent cations. To obtain an adequately buffered, nonprecipitating Zn^{2+} solution, a 150 mM choline-Cl solution was pH adjusted to 7.6 using TRIS base and HCl, followed by addition of 10 mM $ZnCl_2$, yielding a final pH of 5.5. We also performed Zn^{2+}-substitution experiments where the cells were kept in a solution containing (in mM): choline-Cl 160, TRIS 10, and $CaCl_2$ 1, pH 7.3. Cells were then superfused with an identical solution, except that 1 mM $CaCl_2$ was replaced by 1 mM $ZnCl_2$ (Fig. 5 A, open circles). Solution changes were performed by pressure ejection from a wide-tipped pipette.

Patch-clamp Experiments

Patch-clamp experiments were performed in the tight-seal whole-cell configuration at 21–25°C. High-resolution current recordings were acquired by a computer-based patch-clamp amplifier system (EPC-9, HEKA). Patch pipettes had resistances between 2–4 MΩ after filling with the standard intracellular solu-

The Journal of General Physiology

tion. Immediately following establishment of the whole-cell configuration, voltage ramps of 50 ms duration spanning the voltage range of −100 to 100 mV were delivered from a holding potential of 0 mV at a rate of 0.5 Hz over a period of 300–400 s. All voltages were corrected for a liquid junction potential of 10 mV between external and internal solutions when using glutamate as intracellular anion. Currents were filtered at 2.9 kHz and digitized at 100 μs intervals. Capacitive currents and series resistance were determined and corrected before each voltage ramp using the automatic capacitance compensation of the EPC-9. In HEK-293 cells overexpressing TRPM7, data were analyzed without correcting for leak currents, since there is a significant level of basal TRPM7 conductance at the time of whole-cell establishment (break-in). The low-resolution temporal development of currents at a given potential was extracted from individual ramp current records by measuring the current amplitudes at voltages of −80 mV and 80 mV, respectively. Where applicable, statistical errors of averaged data are given as means ± SEM with n determinations and statistical significance was assessed by Student's t test.

Fluorescence Measurements and Divalent-induced Quench of Fura-2

Cytosolic calcium concentration of patch-clamped cells was monitored at a rate of 5 Hz with a photomultiplier-based system using a monochromatic light source (TILL Photonics) tuned to excite fura-2 fluorescence at 360 and 390 nm for 20 ms each. Emission was detected at 450–550 nm with a photomultiplier whose analogue signals were sampled and processed by the X-Chart software package (HEKA). Fluorescence ratios were translated into free intracellular calcium concentration based on calibration parameters derived from patch-clamp experiments with calibrated calcium concentrations. A standard Ringer's solution was used except that Ca^{2+} was increased to 2 mM. In patch-clamp experiments, 200 μM Fura-2 was added to the standard intracellular solution without BAPTA. In some cases, 3 mM Mg·ATP was added to suppress TRPM7. For Mn^{2+}-, Co^{2+}-, or Ni^{2+}-induced fluorescence quenching, intact cells were loaded with 5 μM fura-2-AM for 45–60 min at 37°C. Fluorescence recordings were initially made in an external solution that was nominally Mg^{2+} free but contained 3 mM extracellular Ca^{2+}. Quenching of the 360 nm signal (the Ca^{2+}-independent wavelength of fura-2) was assessed during application of a Ringer's solution containing either 1 mM of $MnCl_2$, $CoCl_2$, or $NiCl_2$ plus both $CaCl_2$ and $MgCl_2$ (1 mM each) via a wide-tipped, pressure-controlled application pipette.

RESULTS

TRPM7 Provides a Significant Ca^{2+} Entry Pathway

As we have shown previously with electrophysiological recordings that TRPM7 allows permeation of Ca^{2+} (Nadler et al., 2001), we assayed $[Ca^{2+}]$i using fura-2 to ascertain that the channel could indeed function as a significant Ca^{2+} influx pathway to cause changes in cytosolic Ca^{2+} levels. To this end, HEK-293 cells overexpressing TRPM7 were kept in a bath solution with 2 mM each of Ca^{2+} and Mg^{2+} and were perfused via the patch pipette with a Cs-glutamate–based internal solution containing 200 μM fura-2 and no other exogenous Ca^{2+} buffers. The simultaneous development of magnesium-nucleotide regulated metal current (MagNuM) was monitored under whole-cell patch-clamp by delivering, from a holding potential of 0 mV, repetitive voltage ramps that spanned −100 to 100 mV over 50 ms at a rate of 0.5 Hz. When Mg·ATP was absent in the pipette, MagNuM rapidly activated, as witnessed by the increase in both inward and outward currents (Fig. 1 A) as well as its characteristic highly nonlinear current-voltage (I-V) relationship (Fig. 1 B, dotted trace). In parallel, fluorescence measurements revealed a steady increase of $[Ca^{2+}]$i (Fig. 1 C) that was due to Ca^{2+} influx, since $[Ca^{2+}]$i transiently increased during periodic 5-s hyperpolarizations to −80 mV ($n = 6$). By contrast, in cells where the internal solution contained 3 mM Mg·ATP, there was little change in TRPM7 activity and $[Ca^{2+}]$i remained similarly steady under these conditions. An example I-V curve under these conditions is shown in Fig. 1 B (solid trace). The progressive decrease in amplitude of hyperpolarization-driven changes in $[Ca^{2+}]$i observed under these conditions is likely due to increased Ca^{2+} buffering as fura-2 equilibrates with the cytosol at its final concentration of 200 μM. Control uninduced cells not overexpressing TRPM7 perfused with ATP-free solutions (dotted trace in Fig. 1 C) behaved very much like TRPM7 overexpressing cells perfused with 3 mM ATP, suggesting that the increase in $[Ca^{2+}]$i is not simply due to compromised pumping activity (although this may account for the small increase observed toward the end of the experiment). Thus, it appears that at physiologic concentrations of extracellular Ca^{2+} and Mg^{2+}, activation of MagNuM allows significant Ca^{2+} entry in cells overexpressing TRPM7.

Equimolar Substitution of 10 mM Extracellular Ca^{2+} by Transition Metals

To assess the permeation of other divalent ions, we measured ionic currents in ion-substitution experiments, where 10 mM Ca^{2+} was replaced with 10 mM of other divalent cations. In these experiments, HEK-293 cells overexpressing TRPM7 were kept in a bath solution containing 10 mM Ca^{2+}, without Mg^{2+}, and development of TRPM7-mediated current was monitored by whole-cell patch-clamp. When the current had reached maximal amplitude, cells were transiently exposed to an extracellular solution containing 10 mM of the test cation applied for a period of 60 s. As illustrated in Fig. 2, this resulted in characteristic changes of TRPM7-mediated inward and outward currents. To better compare the responses and compensate for variations in expression levels, we normalized both outward and inward currents such that the current magnitudes just before substituting Ca^{2+} were set to 1. The changes in inward current are therefore relative to the current magnitude of 10 mM Ca^{2+}.

The Journal of General Physiology

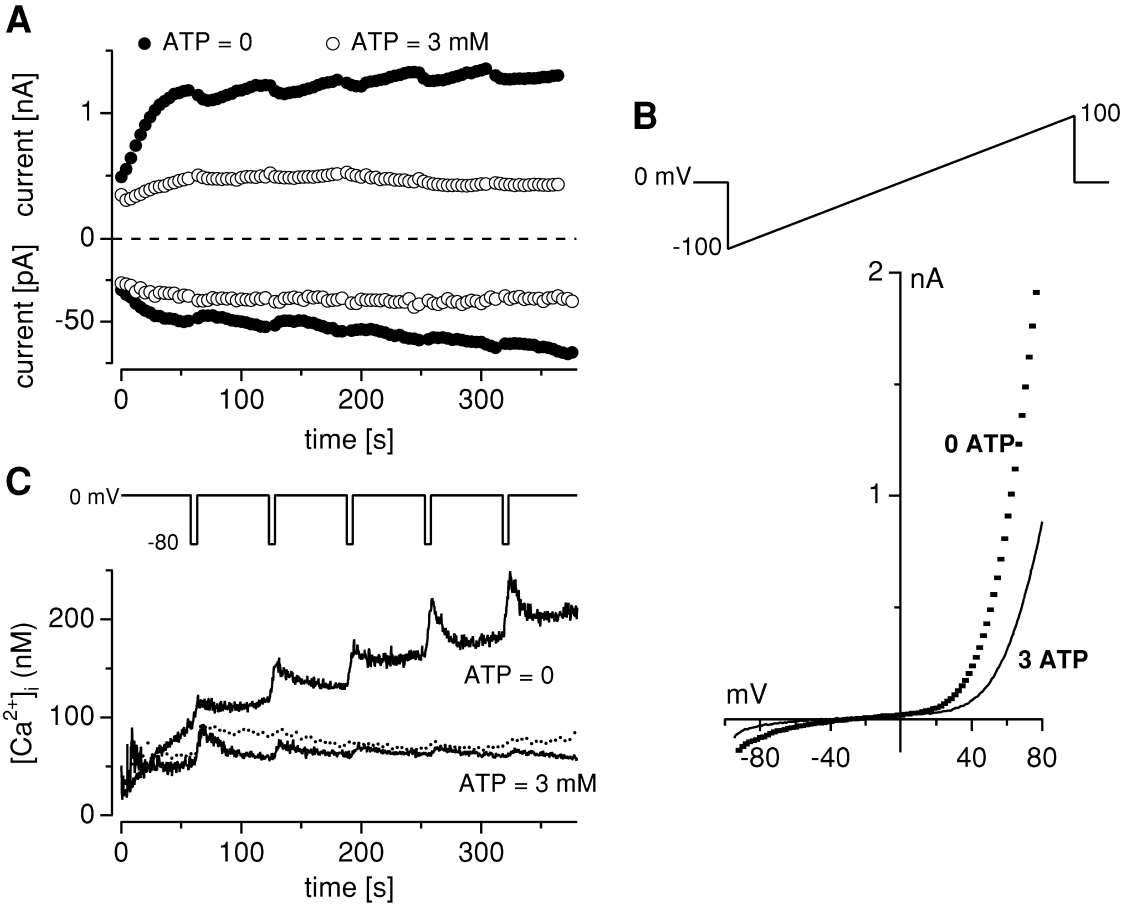

FIGURE 1. TRPM7 is an influx pathway for Ca^{2+}. Simultaneous whole-cell patch-clamp recordings of MagNuM and fura-2 measurements of $[Ca^{2+}]i$ in HEK-293 cells overexpressing TRPM7. (A) Average inward and outward MagNuM currents at −80 and 80 mV, respectively, in cells perfused with Cs-glutamate–based internal solution in the absence of Mg·ATP (filled circles, $n = 6$) and with 3 mM Mg·ATP (open circles, $n = 6$). Note the different Y-axis scaling. (B) Representative high-resolution current record obtained in response to a 50-ms voltage ramp from −100 to 100 mV from a cell dialyzed with 0 Mg·ATP or 3 mM Mg·ATP, respectively, showing the characteristic signature of MagNuM (strong outward rectification at potentials above 40 mV and suppression by increased Mg·ATP concentrations). Note that data are not leak-corrected which reveals a reversal potential of −33.2 mV ± 2.4 mV ($n = 9$) under conditions where intracellular calcium is weakly buffered. (C) Average intracellular Ca^{2+} signals recorded from cells patched in A showing a steady rise in $[Ca^{2+}]i$ in the absence of Mg·ATP. In contrast, $[Ca^{2+}]i$ remains at steady basal levels when TRPM7 is blocked by 3 mM Mg·ATP or in control uninduced HEK-293 cells not overexpressing the channel (dotted line, $n = 5$).

As shown in Fig. 2 A, Zn^{2+} and Ni^{2+} caused a large increase of the inward current, combined with a block of outward currents. For both Zn^{2+} and Ni^{2+}, the increase in inward current was greater than threefold compared with Ca^{2+} (Fig. 2 D), whereas the inhibition of outward currents was less pronounced for Zn^{2+} than for Ni^{2+}. Ba^{2+} was able to sustain significant inward currents (Fig. 2 B, right, and D), but without suppression of outward currents. Co^{2+}, Mg^{2+}, and Mn^{2+} are characterized by more modest (less than double) increases of inward currents, but were again accompanied by a block of outward currents (Fig. 2 B, left, and D). The strongest block of outward currents was caused by Mg^{2+}, which we have previously shown is a strong independent suppressor of MagNuM currents (Nadler et al., 2001; Hermosura et al., 2002). Ba^{2+}, Sr^{2+}, and Cd^{2+} application increased the outward current with only slight to moderate increases of the inward current (Fig. 2, C and D).

In the experiments described above, where we substituted 10 mM Ca^{2+} with other divalent ions, one would expect the reversal potential (E_{rev}) to shift at least to some degree toward depolarized potentials. Indeed, this could be observed for all ion species investigated. Compared with control E_{rev} values (−7.2 ± 2.7 mV; $n = 39$), Ba^{2+} and Ni^{2+} had the strongest effect in shifting E_{rev} by 19 ± 7, ($n = 5$) and 15 mV ± 3 ($n = 6$), respectively. At 10 mM concentration, the other ion species investigated had less dramatic effects, ranging between 2 mV ± 0.7 mV for Cd^{2+} ($n = 5$) and 8.5 mV ± 4.7 mV for Co^{2+} ($n = 5$). Example I-V curves are shown in Fig. 2 C. Here a cell was superfused with a 10 mM Ni^{2+}-containing extracellular Mg^{2+}-free solution. The currents

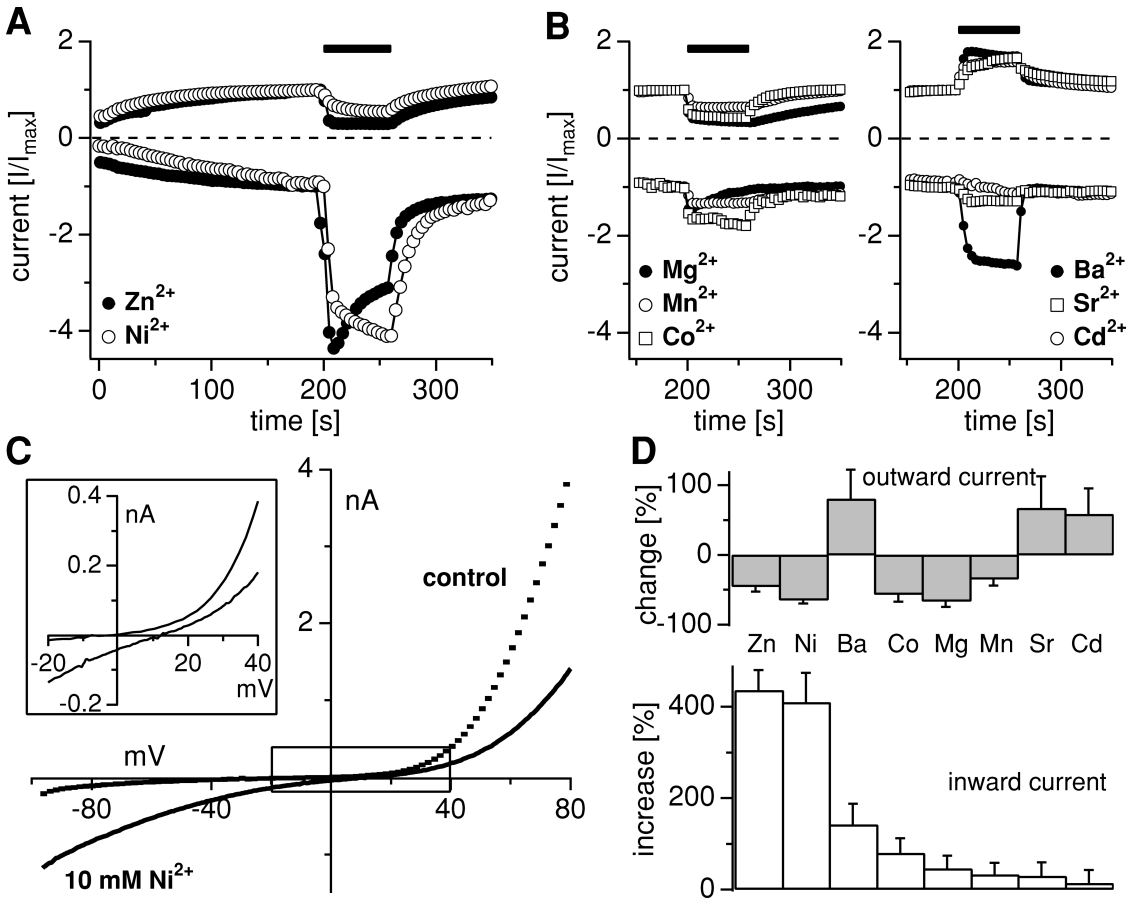

FIGURE 2. Equimolar substitution of 10 mM Ca^{2+} by transition metals. Whole-cell currents were recorded in HEK-293 cells overexpressing TRPM7 kept in a bath containing 10 mM Ca^{2+}, without Mg^{2+}, and exposed for 60 s to an otherwise identical external solution where 10 mM Ca^{2+} was equimolarly replaced by the test cation. Average inward and outward currents at −80 and 80 mV were scaled so that the inward and outward current amplitudes immediately preceding the solution change were set to 1. (A) Exposure to 10 mM Zn^{2+} ($n = 5$) and 10 mM Ni^{2+} ($n = 9$) caused a large increase of the inward current, with a block of the outward current. (B) Left, 10 mM Co^{2+} ($n = 3$), 10 mM Mg^{2+} ($n = 5$), and 10 mM Mn^{2+} ($n = 5$) caused a slight to moderate increase of the inward current, with a block of the outward current. Right, 10 mM Ba^{2+} ($n = 6$), 10 mM Sr^{2+} ($n = 3$), and 10 mM Cd^{2+} ($n = 3$) caused a slight to moderate increase of the inward current, and increase of the outward current. Note that the first 150 s of whole-cell time are not shown. (C) Representative high-resolution current record obtained in response to a 50-ms voltage ramp from −100 to 100 mV from a cell before (200 s whole-cell time, dotted control) and during (250 s whole-cell time, thick continuous line) application of 10 mM Ni^{2+} showing the right shift in reversal potential during application. Note that data are not leak-corrected, which reveals an average control reversal potential of −7.2 mV ± 2.7 mV ($n = 39$) under conditions where intracellular calcium is buffered to zero. The black open box indicates the area shown enlarged in the inset to the left. (D) The bottom panel shows the rank order of permeation through TRPM7 based on percentage increase (±SEM) of the inward current when carrying the test cation relative to the current magnitude at 10 mM Ca^{2+}. The top panel plots effects on the outward current as percent increase or inhibition (±SEM) for each divalent cation.

just before application (at 200 s whole-cell time) and during application (at 230 s) are shown. It can be seen that there is a remarkable increase in inward currents with some suppression of the outward current. This is accompanied by a clear depolarizing shift of E_{rev}, as detailed by the magnified inset. However, as will be discussed later, a quantitative assessment of reversal potentials under these conditions is rather difficult and error prone, because the current is highly nonlinear and has a very shallow slope around E_{rev}, so that relatively small changes in TRPM7 current and/or Ca^{2+}-dependent conductances may shift it.

Permeation Profile of Transition Metals in Isotonic Solutions

The above experiments reveal the surprising finding that TRPM7 is not only permeable to Ca^{2+} ions, but in fact even more permeable to a range of divalent transition metal ions and their permeation yields considerable macroscopic inward currents at negative membrane potentials. It should be noted, however, that the above experiments cannot unequivocally rule out possible ion–ion interactions that would allow the cotransport of, e.g., Na^+ ions along with divalent ions. To avoid such complications, we next studied permeation of di-

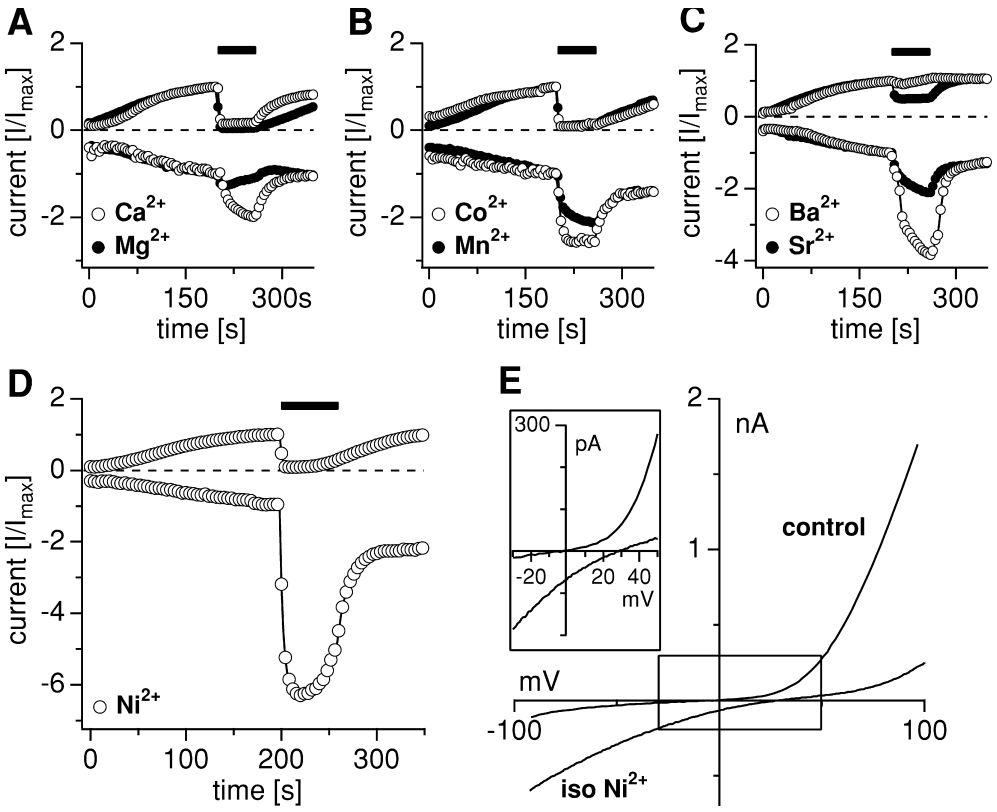

FIGURE 3. Permeation of transition metals in isotonic solutions. Whole-cell currents were recorded in HEK-293 cells overexpressing TRPM7 in standard external solution containing 1 mM Ca^{2+} and 2 mM Mg^{2+}, and subsequently exposed to an isotonic solution of the test cation for 60 s. Average inward and outward currents at −80 and 80 mV were scaled so that the inward and outward current amplitudes immediately preceding the solution change were set to 1. (A–D) Exposure to isotonic Ca^{2+} ($n = 4$), Mg^{2+} ($n = 5$), Co^{2+} ($n = 3$), Mn^{2+} ($n = 5$), Ba^{2+} ($n = 3$), Sr^{2+} ($n = 7$), and Ni^{2+} ($n = 4$) elicits characteristic responses for each cation. Data for Ca^{2+} and Mg^{2+} reprinted in normalized form by permission from *Nature* [Nadler et al., 2001], copyright 2001 Macmillan Publishers Ltd. (E) Representative high-resolution current records obtained in response to a 50-ms voltage ramp from −100 to 100 mV from a cell before (control at 200-s whole-cell time) and during (230-s whole-cell time) exposure to isotonic Ni^{2+} illustrating the right shift in the reversal potential. Note that data are not leak-corrected which reveals an average control reversal potential of −7.2 ± 2.7 mV ($n = 39$) under conditions where intracellular calcium is buffered to zero. The black open box indicates the area shown enlarged in the inset to the left.

valent ions in isotonic extracellular solutions of each metal ion. Isotonic solutions of 120 mM of each divalent ion species yielded appropriate osmolarities within 10% of the standard bath and pipette solutions and pH values in the range of 5.1 to 5.5, which do not compromise accurate assessment of inward currents carried by TRPM7 (see MATERIALS AND METHODS). However, Zn^{2+} and Cd^{2+} had to be excluded from this analysis, as isotonic solutions of Zn^{2+} yielded pH values below 3 and 120 mM Cd^{2+} solutions were hypoosmotic.

In this series of experiments, the cells were initially bathed in the standard external solution containing 1 mM Ca^{2+} and 2 mM Mg^{2+}. At 200 s, when TRPM7 current had reached its full amplitude, isotonic solutions of each metal ion were applied for 60 s via a puffer pipette. The development of inward and outward currents before, during, and after application of selected isotonic divalent cation solutions are shown in Fig. 3 A for the case of Ca^{2+} and Mg^{2+}. The experiments illustrate that isotonic Ca^{2+} and Mg^{2+} solutions induce an increase in inward currents through TRPM7, while at the same time there is strong suppression of outward currents. We next performed essentially identical experiments for a range of divalent metal ions and illustrate the average responses in Fig. 3, B–D. Example I-V curves measured before (200 s whole-cell time) and during isotonic Ni^{2+} application (at 230 s) are shown in Fig. 3 E. Note the dramatic increase in inward currents, the substantial reduction of the outward currents, and the significant depolarizing shift of E_{rev}, which is detailed in the data inset of the graph. When analyzing these data for the relative increase of inward currents, it can be seen that, with the exception of Mg^{2+}, the rank order of permeation under isotonic conditions (Fig. 4, A and B) is virtually identical with the permeation sequence observed in the 10 mM ion substitution experiments (Fig. 2 D).

The analysis of E_{rev} changes induced by isotonic ion application reveals that, similarly to the 10 mM ion substitution experiments, Ni^{2+} induced the strongest depolarizing shift (35.4 ± 2.7 mV, $n = 4$, $P >> 0.001$; Fig. 4 C). Similarly, Mg^{2+} caused the weakest potential change (+10 ± 8 mV, $n = 4$; Fig. 4 C). The effects of the other ions ranked in between those two extremes. It should be noted that the data used for current and reversal potential analysis were not leak subtracted and are relative measurements.

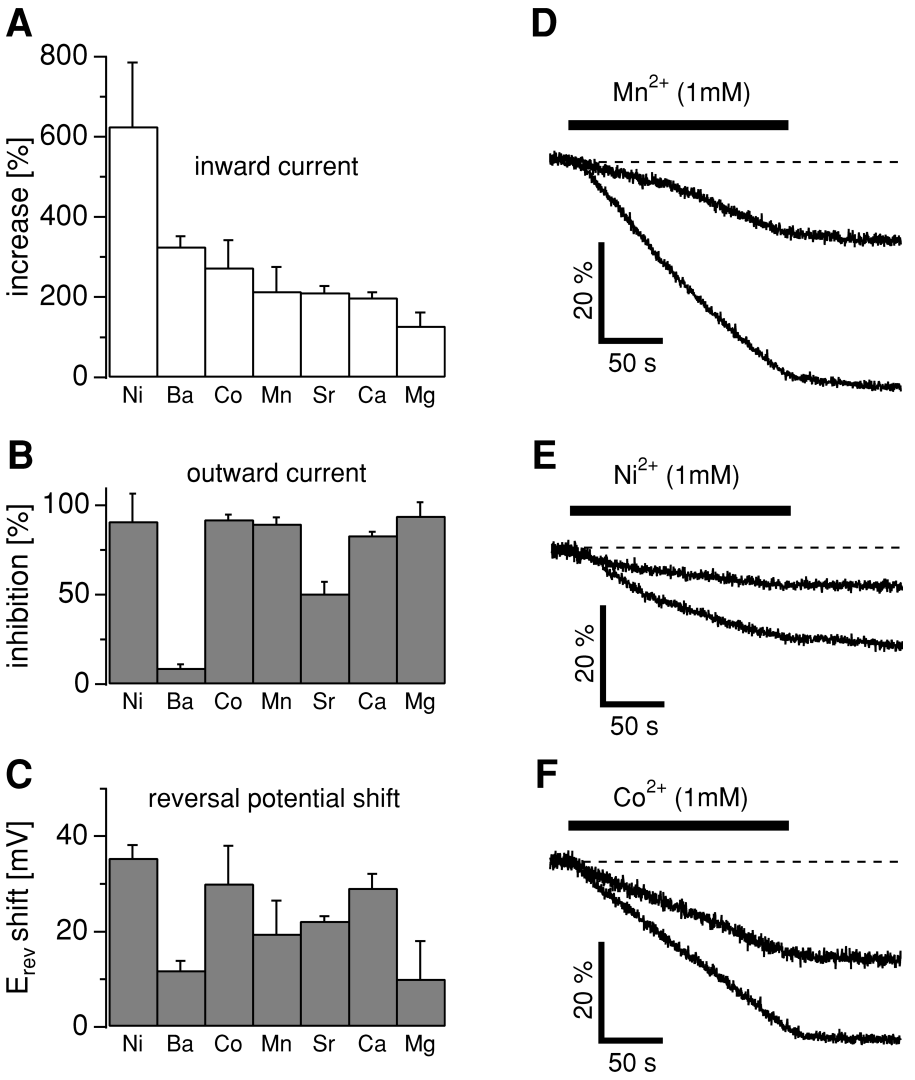

FIGURE 4. (A) The rank order of permeation through TRPM7 based on percentage increase (±SEM) of the peak inward current. Note that increases are relative to 1 mM Ca^{2+}. (B) Corresponding effects on the outward current as percent inhibition (±SEM). (C) Relative shift of reversal potential (E_{rev}) to control E_{rev} (see below) induced by application of the respective isotonic divalent solutions. Data are sorted according to the rank order of inward current (A). The average control reversal potential before application was −7.5 mV ± 5 mV (n = 31) as indicated in Fig. 3 E. (D) Mn^{2+}-induced quench of fura-2 fluorescence at 360 nm excitation in HEK-293 cells induced to overexpress TRPM7 (n = 3) and transfected cells that remained uninduced (n = 3). Cells were kept in an extracellular solution supplemented with 3 mM Ca^{2+} and 0 Mg^{2+}. The application contained 1 mM Mn^{2+}, 1 mM Ca^{2+}, and 1 mM Mg^{2+} as divalent ions. (E) Ni^{2+}-induced quench of fura-2 fluorescence at 360 nm excitation in HEK-293 cells induced to overexpress TRPM7 (n = 4) and control cells that remained uninduced (n = 3). Cells were kept in an extracellular solution as described in Fig. 4 D. The application contained standard solution with 1 mM Ni^{2+}, 1 mM Ca^{2+}, and 1 mM Mg^{2+} as divalent ions. (F) Co^{2+}-induced quench of fura-2 fluorescence at 360 nm excitation in HEK-293 overexpressing TRPM7 (n = 3) and in uninduced control cells (n = 3). Cells were kept in an extracellular solution as described in Fig. 4 D. The application contained standard solution with 1 mM Co^{2+}, 1 mM Ca^{2+}, and 1 mM Mg^{2+} as divalent ions.

The Journal of General Physiology

Physiological Ca^{2+} Levels Do Not Impede Trace Metal Permeation Through TRPM7

TRPM7 mediates low levels of homeostatic plasma membrane Ca^{2+} fluxes and several Ca^{2+} influx pathways are known to also allow permeation of Mn^{2+} ions (Shuttleworth and Thompson, 1999). Therefore, we hypothesized that TRPM7, if it carried Mn^{2+} as well, may underlie experimental observations of unstimulated Mn^{2+} entry that lead to fluorescence quenching of fura-2 in resting cells (Mertz et al., 1990; Shuttleworth and Thompson, 1996). If this were the case, it would also hand us a tool to test whether the presence of physiological Ca^{2+} and Mg^{2+} concentrations, the major divalent ion species in extracellular fluids, affect the permeation of other divalent ions through TRPM7 channels.

To test these hypotheses, HEK-293 cells overexpressing TRPM7 as well as control cells were loaded with fura-2-AM and bathed in the standard external solution containing 3 mM Ca^{2+} and 0 mM Mg^{2+}. Fluorescence was monitored at 360 nm excitation (the isosbestic or Ca^{2+}-independent wavelength of fura-2) and after 20 s, an external solution that maintained the total divalent concentration but contained 1 mM Mn^{2+}, 1 mM Ca^{2+}, and 1 mM Mg^{2+} was applied for 180 s. As shown in Fig. 4 D, the application of 1 mM Mn^{2+} caused a pronounced quench of the 360 nm signal in HEK-293 cells induced to overexpress TRPM7 (n = 3), whereas Mn^{2+}-induced quench of the 360-nm signal in uninduced cells, which express only low levels of endogenous TRPM7, was much less dramatic (n = 3). Linear regression over the initial 60 s of Mn^{2+} exposure yielded a fourfold higher rate of Mn^{2+}-induced quench of fura-2 fluorescence in induced cells (28%/min) as compared with uninduced cells (6.6%/min).

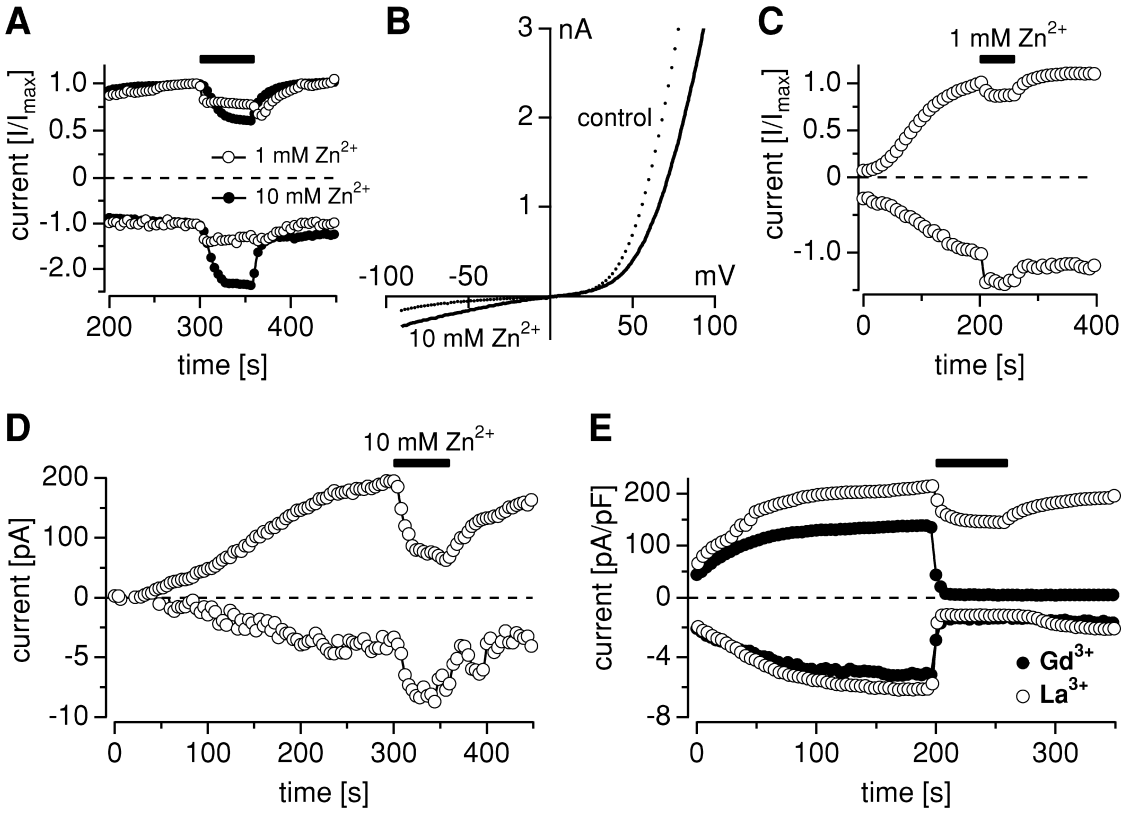

FIGURE 5. Permeation of zinc. (A) Whole-cell currents were recorded in HEK-293 cells overexpressing TRPM7. Closed circles indicate cells that were kept in standard external solution containing 10 mM Ca^{2+} and 0 mM Mg^{2+}, and subsequently exposed to a choline-Cl_2 based solution containing 10 mM Zn^{2+} ($n = 8$). Open circles show cells that were kept in a solution that contained 160 mM choline-Cl, 10 mM TRIS, and 1 mM Ca^{2+} ($n = 5$). During the time indicated by the black bar, cells were superfused with an otherwise identical solution, except that 1 mM Ca^{2+} was replaced with 1 mM Zn^{2+}. Average inward and outward currents at −80 and 80 mV were normalized so that the inward and outward current amplitudes immediately preceding the solution change were set to 1. (B) High-resolution current records from a representative cell showing current-voltage relationships just before (control) and immediately after application of 10 mM Zn^{2+} solution. (C) Whole-cell currents were recorded in WT HEK-293 cells with experimental protocol as in (Fig. 2). Two datasets were generated (a) MagNuM was activated in the absence of Mg·ATP ($n = 12$) and (b) MagNuM was suppressed by 4 mM Mg^{2+} ($n = 5$) Datasets were averaged and subtracted to compensate for Zn^{2+} inhibition of background currents (see text). Note the different Y-axis scaling. (D) Average inward and outward currents at −80 and 80 mV, respectively, recorded in HEK-293 cells overexpressing TRPM7 in standard external solution containing 10 mM Ca^{2+} without Mg^{2+}. 10 mM Gd31 ($n = 3$) or La31 ($n = 6$) were applied as indicated. Note the different Y-axis scaling.

Similar experiments were performed for Ni^{2+}, where an external solution containing 1 mM Ni^{2+}, 1 mM Ca^{2+}, and 1 mM Mg^{2+} was applied for 180 s. Fig. 4 E confirms that Ni^{2+} too can permeate TRPM7 in the presence of Ca^{2+} and Mg^{2+}. Here, the fura-2-induced fluorescence quench increases about twofold from 10%/min in uninduced cells ($n = 3$) to 20%/min in TRPM7 overexpressing cells ($n = 4$). Finally, using Co^{2+} in the presence of Ca^{2+} and Mg^{2+} also increases the rate of fura-2 fluorescence quenching (by about threefold) in TRPM7 overexpressing cells (17%, $n = 3$; Fig. 4 F) versus uninduced controls (5.4%, $n = 3$). These results clearly suggest that basal, unstimulated TRPM7 activity in intact cells constitutes an important pathway for Mn^{2+}, Co^{2+}, and Ni^{2+} entry that is significantly augmented by TRPM7 overexpression and can occur in the presence of physiological levels of Ca^{2+} and Mg^{2+}.

Permeation of Zn^{2+} and Trivalent Ion Species

Based on its physiological and pathophysiological importance, we wanted to ascertain that Zn^{2+} permeation of TRPM7 occurs under experimental conditions in which it was the only permeable ion species available to carry inward currents through TRPM7 channels. As the pH of isotonic Zn^{2+} solutions precluded such experiments, we used the same experimental approach as in Fig. 2, but tested Zn^{2+} permeation by applying 10 mM Zn^{2+} in a choline-Cl–based extracellular solution (see MATERIALS AND METHODS). As illustrated in Fig. 5 A, this resulted in a significant enhancement of inward currents in HEK-293 cells overexpressing TRPM7, indi-

cating that Zn^{2+} is indeed a highly permeable ion species of TRPM7. The current-voltage relationships of TRPM7 before and during Zn^{2+} application are illustrated in Fig. 5 B, demonstrating the increase in inward current at negative potentials and the decrease in outward currents at positive potentials, consistent with significant Zn^{2+} permeation. To further confirm Zn^{2+} permeation in the absence of other permeant ion species, we performed experiments where TRPM7-overexpressing cells were kept in a choline-Cl–based solution supplemented with 1 mM Ca^{2+} instead of our standard external solution (see MATERIALS AND METHODS; Fig. 5 A, open circles, $n = 5$). At the time indicated, patch-clamped cells were then superfused with 1 mM Zn^{2+} and 0 mM Ca^{2+} in an otherwise identical choline-Cl solution. The results show that even at 1 mM concentration, Zn^{2+} alone is more effective in supporting inward current than equimolar Ca^{2+}.

We also attempted to measure Zn^{2+} permeation under more physiological conditions, i.e., in the presence of physiological Ca^{2+} and Mg^{2+} concentrations. To this end, we allowed TRPM7 currents to develop in standard extracellular solutions containing 1 mM Ca^{2+} and 2 mM Mg^{2+} and applied the same solution, but additionally contained 1 mM Zn^{2+}. Under these conditions, we again observed a clear increase in inward current and a concomitant small decrease in outward current (Fig. 5 C), suggesting additive permeation of Zn^{2+} ions in the presence of Ca^{2+} and Mg^{2+}.

Finally, to address the issue of whether Zn^{2+} permeation is also characteristic of native, endogenously expressed TRPM7, we recorded MagNuM in wild-type (WT) HEK-293 cells under identical conditions as the ion-substitution experiments in Fig. 2, with 10 mM Zn^{2+} as the replacement ion. Since Zn^{2+} inhibits resting background currents unrelated to TRPM7, we corrected for this effect by first measuring Zn^{2+} effects in cells where MagNuM was completely suppressed by pipette solutions containing 4 mM Mg^{2+} ($n = 5$). These data were averaged and subtracted from the average dataset obtained from cells where MagNuM was activated by omission of pipette Mg·ATP ($n = 12$). As can be seen in Fig. 5 D, we observed a significant increase in inward current when applying Zn^{2+}, indicating that Zn^{2+} permeation is a genuine physiological property of native TRPM7 channels.

We also tested for permeation of trivalent metal ions La^{3+} and Gd^{3+} (Fig. 5 E). We first assessed concentrations that normally completely suppress voltage- or store-operated Ca^{2+} channels and found that 10 μM of either Gd^{3+} or La^{3+} were rather ineffective in suppressing inward or outward currents carried by TRPM7 (<5% inhibition, $n = 3$–4, unpublished data). However, at 10 mM, both ions almost completely inhibited inward currents ($n = 5$ each), although the effects on outward currents were markedly different. Provided that the inhibitory action of Gd^{3+}, and to a smaller degree that of La^{3+}, is mediated at the cytosolic side, there may in fact be a very small permeation of this ion that cannot be unambiguously resolved at the macroscopic current level.

DISCUSSION

The main result of the present study is that the widely expressed ion channel TRPM7, which has previously been shown to conduct both Ca^{2+} and Mg^{2+} (Nadler et al., 2001) is permeable to a variety of divalent cations with a permeability sequence of $Zn^{2+} \approx Ni^{2+} >> Ba^{2+} > Co^{2+} > Mg^{2+} \geq Mn^{2+} \geq Sr^{2+} \geq Cd^{2+} \geq Ca^{2+}$ and they do so even in the presence of physiological levels of Ca^{2+} and Mg^{2+}. Our results therefore suggest that TRPM7 represents a novel and unique ion-channel pathway for cellular divalent ion transport.

TRPM7 Constitutes a Significant Ca^{2+} Entry Pathway

Previous electrophysiological characterizations of TRPM7 have established that the channel is capable of sustaining small inward currents carried by Ca^{2+} ions (Nadler et al., 2001; Runnels et al., 2001). We have extended this analysis in the present work by combined fluorescence and patch-clamp measurements (see Fig. 1), which demonstrate that TRPM7 can drive significant changes in $[Ca^{2+}]i$ after depletion of intracellular Mg·ATP in cells that overexpress the protein. In native cells, where expression levels of endogenous TRPM7 is smaller, the contribution of MagNuM may be more subtle and may not lead to measurable changes of free $[Ca^{2+}]i$. However, given that TRPM7 is constitutively active to a small degree, even in the presence of physiological Mg·ATP, it can well serve a function of a homeostatic mechanism for basal, background influx of Ca^{2+} that could be used to maintain the filling state of intracellular stores. The notion that MagNuM constitutes a background pathway for divalent cation fluxes is supported by the fluorescence quenching experiments illustrated in Fig. 4, where a small basal entry of Mn^{2+}, Co^{2+}, and Ni^{2+} is observed in intact uninduced cells, which is presumably due to native MagNuM and is augmented significantly in cells overexpressing TRPM7. From this, it seems reasonable to assume that the same pathway can support a steady, low-level transport of Ca^{2+} ions, which under extreme conditions, such as prolonged ischemia, can lead to a persistent strong activation of TRPM7 that ultimately may contribute to Ca^{2+} overload and cell death.

Equimolar Substitution of 10 mM Extracellular Ca^{2+} by Transition Metals

In general, all tested divalent metal ions were at least as efficient and some even considerably more so than Ca^{2+} in permeating TRPM7 at negative membrane po-

The Journal of General Physiology

tentials. Zn^{2+} and Ni^{2+} caused the largest increases of the inward current, which were greater than threefold compared with Ca^{2+}. We also observed significant Ba^{2+} inward currents, while Co^{2+}, Mg^{2+}, and Mn^{2+} exhibit more modest (less than double) increases of inward currents and Sr^{2+} and Cd^{2+} still supported slightly larger inward currents than Ca^{2+} itself. Taken together, the changes in inward current observed under 10 mM ion substitution experiments are most consistent with the interpretation that TRPM7 is as or more permeable to each of the divalent cations than Ca^{2+}.

At the same time, most of these ions produced a significant block of outward currents, the strongest one caused by Mg^{2+}, which we have shown previously is a potent intracellular suppressor of MagNuM currents (Nadler et al., 2001; Hermosura et al., 2002). In contrast, Ba^{2+}, Sr^{2+}, and Cd^{2+}, while still supporting inward currents, actually increase outward currents. The outward currents at positive potentials represent currents of monovalent ions at potentials where divalent ions do not experience sufficient driving force to enter the cell and therefore no longer impede monovalent outward fluxes (Hille, 1992). Their behavior is a complex function of several factors including (a) the Nernst equilibrium potential of divalent ions, which determines the degree of permeation block imposed by divalent ions at positive membrane potentials, and (b) inhibitory effects of the relevant divalent ion at the intracellular side of the channel after it has gained access to the cytosol. The latter effects are particularly relevant for Mg^{2+}, which plays an important role as a cofactor in the gating of TRPM7 and therefore can inactivate MagNuM if allowed to accumulate intracellularly. A similar inhibition is also seen with Ca^{2+}, which is the second major physiological divalent cation to permeate TRPM7. However, under our experimental conditions, the inhibitory action of $[Ca^{2+}]i$ may be more limited due to the inclusion of 10 mM BAPTA and may be only noticeable under the weakly buffered conditions during calcium signaling measurements (e.g., Fig. 1). Based on the inhibitory actions of a number of divalent ions, we propose putative divalent binding site(s) at the cytosolic side of TRPM7 that modify channel gating and/or cause channel block. Different divalent ions may possess different affinities to this site, resulting in the observed inhibition of outward currents. Thus, the efficacy of any divalent ion to block outward currents would be the net result of its degree of permeation, its ability to accumulate in the cytosol in the presence of BAPTA, and its inhibitory potency on the channel.

Permeation of Transition Metals in Isotonic Solutions

In general agreement with the 10 mM substitution experiments, application of isotonic divalent solutions resulted in increased inward currents and inhibition of outward currents. The permeation sequence of divalent ions, based on peak inward currents, is similar to the sequence we observed with 10 mM ion-substitution experiments. Thus, in the absence of data for isotonic Zn^{2+}, Co^{2+} and Mn^{2+} are the best-permeating physiologically relevant metal ions, followed by Ca^{2+} and Mg^{2+}. Among the toxic or nonphysiologic metals, Ni^{2+} is the most permeable, followed by Ba^{2+} and Sr^{2+}. This permeation sequence, in combination with the facilitated transport of trace metals over Ca^{2+} and Mg^{2+}, is unprecedented for any ion channel presently known. TRPM7 must therefore be considered an important influx pathway for both essential and toxic metal ions. With respect to outward currents, isotonic solutions invariably caused a complete or almost complete inhibition, with the exception of Ba^{2+} and Sr^{2+}, which were less effective in doing so. As in the equimolar substitution experiments, here too the efficacy of permeation and its rank order would be a net result of the three factors discussed above (permeation, intracellular ion accumulation and negative feedback on the channel). In most cases, the currents recovered close to their original sizes within ~150 s, suggesting that none of the divalent ion species exert any lasting effect on channel integrity.

Together, both datasets (10 mM equimolar replacements and isotonic substitutions) are complementary in that they address interpretation issues that arise under either experimental condition. For example, the acidic nature of isotonic divalent solutions prevented us to conduct experiments with isotonic Zn^{2+}. This was not a concern with the 10 mM replacement experiments. Most importantly, however, the two datasets show that in the case of TRPM7, the rank order of the permeation sequence is essentially independent of the divalent ion concentration and the presence of monovalent cations (Na^{+}). The latter aspect is in marked contrast to observations made with other channels that are able to conduct divalent ions other than Ca^{2+}.

Trace Metal–induced Current Augmentation Shifts E_{rev}

Ion permeation ratios are usually calculated based on reversal potentials using Nernst and Goldmann-Hodgkin-Katz (GHK) equations (Hille, 1992), which make the important implicit assumption that ions can permeate independently. Applying this formalism to TRPM7 currents, which normally reverse around 0 mV, would lead to the conclusion that the channel is nonselective (Runnels et al., 2001). However, since TRPM7 conducts divalent ions into the cell and monovalent ions out of the cell (Nadler et al., 2001), the independence rule is questionable and, therefore, correct permeability ratios based on GHK-based calculations do not adequately describe this channel's permeability. Nevertheless, if other ions preferentially permeate

The Journal of General Physiology

TRPM7 over Ca^{2+}, one would expect a depolarizing shift in the reversal potential when applying the 10 mM equimolar or isotonic replacement solutions. Indeed, analyses of reversal potentials revealed that all divalent ions caused a shift in E_{rev} toward more positive potentials. The rank order of the E_{rev} values under isotonic conditions fairly well reflected the rank order observed for the inward currents, with Ni^{2+} inducing the strongest change (35 mV) and Mg^{2+} the weakest (10 mV). This indicates that unlike observations made in other channels (Adams et al., 1980) the apparent permeability of TRPM7 for divalent ions is independent of their concentration.

Reversal potential measurements of TRPM7 are clearly very difficult, because the current is highly nonlinear and has a very shallow slope around E_{rev}. Therefore, even small changes in the activity of other ion currents may have an effect on E_{rev}. In particular, we have noticed that the current magnitude as well as E_{rev} of TRPM7 is influenced by intracellular Ca^{2+} concentrations. In experiments where intracellular Ca^{2+} remained largely unbuffered (e.g., Fig. 1 B), there is a slight shift of the apparent E_{rev} to more hyperpolarized potentials (−33 mV) compared with standard conditions in which $[Ca^{2+}]i$ is buffered to zero using 10 mM Cs-BAPTA (here, E_{rev} values are around −7.2 mV, Fig. 2 C). We have not assessed the reasons for this shift, but we suspect that elevated $[Ca^{2+}]i$ may cause small increases in Ca^{2+}-activated K^+ or Cl^- channels, which may account for the observed changes in E_{rev}.

TRPM7-mediated Trace Metal Entry Occurs at Physiological Levels of Ca^{2+} and Mg^{2+}

Our present work extends our previous observation that TRPM7 sustains Ca^{2+} and Mg^{2+} currents under isotonic conditions (Nadler et al., 2001) by demonstrating other divalent ions to do so. An important question is whether these divalent ions permeate TRPM7 in the presence of physiological levels of extracellular Ca^{2+} and Mg^{2+}? Our results presented in Fig. 4 demonstrate that physiological concentrations of Ca^{2+} and Mg^{2+} do not impede the permeation of Mn^{2+}, Ni^{2+}, or Co^{2+}, providing strong evidence that neither Ca^{2+} nor Mg^{2+} interfere with the permeation of trace metal ions and that divalent ions permeate independently. Thus, the probability of a trace metal ion to pass through the channel would depend on its relative permeability and relative concentration levels. For example, the data in Fig. 2 D show that Zn^{2+} has a fourfold higher chance over Ca^{2+} to permeate TRPM7. Thus, one can presume that under physiological divalent concentrations (i.e., 1 mM Ca^{2+}, 1 mM Mg^{2+}, and 10 μM Zn^{2+} plasma levels; Perveen et al., 2002), ∼1 in every 50 ions passing through the channel will be a Zn^{2+} ion.

Permeation of Zn^{2+} and Trivalent Ion Species

Zn^{2+} plays an important physiological role in many cellular functions. Our results under experimental conditions where Zn^{2+} is the only permeable ion species available to support inward currents through TRPM7 channels demonstrate that Zn^{2+} permeates TRPM7 at least twice as well as Ca^{2+}, indicating unequivocally that Zn^{2+} is indeed a highly permeable ion species of TRPM7. Moreover, this finding could be confirmed in native TRPM7-like MagNuM currents. In the brain, Zn^{2+} levels can reach 100–500 μM during ischemia, making TRPM7 an attractive candidate for mediating at least part of the severe neurotoxic effects observed with this ion (Choi and Koh, 1998; Koh, 2001), particularly in view of the fact that Mg·ATP levels during ischemia are reduced and would favor activation of MagNuM.

Although TRPM7 clearly allows passage of divalent ions, the situation is less clear for trivalent ion influx. Generally, trivalent ions such as Gd^{3+} or La^{3+} are known to efficiently inhibit voltage- or store-operated Ca^{2+} channels at μM concentrations. However, when testing these two ion species, we found that 10 μM of either Gd^{3+} or La^{3+} were rather ineffective in suppressing inward or outward currents carried by TRPM7. At 10 mM concentrations, both ions completely inhibited inward currents with no sign of significant permeation. Interestingly, Gd^{3+} caused a complete suppression of outward currents. It remains to be determined whether this is due to some limited Gd^{3+} entry that causes block of outward currents from the cytosolic side. By contrast, the same concentration of La^{3+}, while potently and persistently inhibiting inward currents, was far less effective in suppressing outward currents, which might be interpreted such that its action is limited to the extracellular side of the plasma membrane.

Conclusions

The present study establishes that the TRPM7 ion channel possesses the so far unique ability to efficiently conduct many nutritionally essential trace metal ions, along with several toxic metal ions as well. This ability in conjunction with its widespread expression and constitutive activity suggests that TRPM7 underlies a ubiquitous mechanism for entry of metal ions into cells. A remarkable finding is that trace divalent metal ions are significantly more permeable through TRPM7 than the dominant physiological divalent metal ions Ca^{2+} and Mg^{2+}. Such a property would help ensure that trace metals are able to effectively compete with these ions and enter into cells despite their concentration disadvantage relative to the millimolar amounts of Ca^{2+} and Mg^{2+} typically present in extracellular fluids. Furthermore, the discovery of the general nature of metal ion

permeation via TRPM7 has important implications for our understanding of pathophysiological situations in which toxicity of TRPM7-permeant ions is thought to play a role. Due to its transport capacity of this and other metal ions, TRPM7 may represent an intriguing target pathway for therapeutic intervention in these situations.

This work was supported in part by National Institutes of Health grants R01-GM65360 to A. Fleig, R01-GM64316 to A.M. Scharenberg, and R01-AI50200, R01-NS40927, to R. Penner.

David Gadsby served as editor.

Submitted: 29 October 2002
Revised: 10 December 2002
Accepted: 11 December 2002

REFERENCES

Adams, D.J., T.M. Dwyer, and B. Hille. 1980. The permeability of endplate channels to monovalent and divalent metal cations. *J. Gen. Physiol.* 75:493–510.

Berridge, M., P. Lipp, and M. Bootman. 1999. Calcium signalling. *Curr. Biol.* 9:R157–R159.

Caterina, M.J., M.A. Schumacher, M. Tominaga, T.A. Rosen, J.D. Levine, and D. Julius. 1997. The capsaicin receptor: a heat-activated ion channel in the pain pathway. *Nature.* 389:816–824.

Choi, D.W., and J.Y. Koh. 1998. Zinc and brain injury. *Annu. Rev. Neurosci.* 21:347–375.

Cousins, R.J., and R.J. McMahon. 2000. Integrative aspects of zinc transporters. *J. Nutr.* 130:1384S–1387S.

Fasolato, C., M. Hoth, G. Matthews, and R. Penner. 1993a. Ca^{2+} and Mn^{2+} influx through receptor-mediated activation of nonspecific cation channels in mast cells. *Proc. Natl. Acad. Sci. USA.* 90:3068–3072.

Fasolato, C., M. Hoth, and R. Penner. 1993b. Multiple mechanisms of manganese-induced quenching of fura-2 fluorescence in rat mast cells. *Pflugers Arch.* 423:225–231.

Fukuda, J., and K. Kawa. 1977. Permeation of manganese, cadmium, zinc, and beryllium through calcium channels of an insect muscle membrane. *Science.* 196:309–311.

Gaither, L.A., and D.J. Eide. 2000. Functional expression of the human hZIP2 zinc transporter. *J. Biol. Chem.* 275:5560–5564.

Gaither, L.A., and D.J. Eide. 2001. The human ZIP1 transporter mediates zinc uptake in human K562 erythroleukemia cells. *J. Biol. Chem.* 276:22258–22264.

Gunshin, H., B. Mackenzie, U.V. Berger, Y. Gunshin, M.F. Romero, W.F. Boron, S. Nussberger, J.L. Gollan, and M.A. Hediger. 1997. Cloning and characterization of a mammalian proton-coupled metal-ion transporter. *Nature.* 388:482–488.

Harris, E.D. 2002. Cellular transporters for zinc. *Nutr. Rev.* 60:121–124.

Harteneck, C., T.D. Plant, and G. Schultz. 2000. From worm to man: three subfamilies of TRP channels. *Trends Neurosci.* 23:159–166.

Hediger, M.A. 1997. Membrane permeability. The diversity of transmembrane transport processes. *Curr. Opin. Cell Biol.* 9:543–546.

Hermosura, M.C., M.K. Monteilh-Zoller, A.M. Scharenberg, R. Penner, and A. Fleig. 2002. Dissociation of the store-operated calcium current I_{CRAC} and the Mg-nucleotide-regulated metal ion current MagNuM. *J. Physiol.* 539:445–458.

Hille, B. 1992. Ionic Channels of Excitable Membranes. Sinauer, Sunderland, MA. 607 pp.

Hoth, M., and R. Penner. 1993. Calcium release-activated calcium current in rat mast cells. *J. Physiol.* 465:359–386.

Jacob, R. 1990. Agonist-stimulated divalent cation entry into single cultured human umbilical vein endothelial cells. *J. Physiol.* 421:55–77.

Kerchner, G.A., L.M. Canzoniero, S.P. Yu, C. Ling, and D.W. Choi. 2000. Zn^{2+} current is mediated by voltage-gated Ca^{2+} channels and enhanced by extracellular acidity in mouse cortical neurones. *J. Physiol.* 528:39–52.

Knopfel, M., G. Schulthess, F. Funk, and H. Hauser. 2000. Characterization of an integral protein of the brush border membrane mediating the transport of divalent metal ions. *Biophys. J.* 79:874–884.

Koh, J.Y. 2001. Zinc and disease of the brain. *Mol. Neurobiol.* 24:99–106.

Lee, J.Y., T.B. Cole, R.D. Palmiter, S.W. Suh, and J.Y. Koh. 2002. Contribution by synaptic zinc to the gender-disparate plaque formation in human Swedish mutant APP transgenic mice. *Proc. Natl. Acad. Sci. USA.* 99:7705–7710.

Merritt, J.E., R. Jacob, and T.J. Hallam. 1989. Use of manganese to discriminate between calcium influx and mobilization from internal stores in stimulated human neutrophils. *J. Biol. Chem.* 264: 1522–1527.

Mertz, L.M., B.J. Baum, and I.S. Ambudkar. 1990. Refill status of the agonist-sensitive Ca^{2+} pool regulates Mn^{2+} influx into parotid acini. *J. Biol. Chem.* 265:15010–15014.

Montell, C., L. Birnbaumer, V. Flockerzi, R.J. Bindels, E.A. Bruford, M.J. Caterina, D.E. Clapham, C. Harteneck, S. Heller, D. Julius, et al. 2002. A unified nomenclature for the superfamily of TRP cation channels. *Mol. Cell.* 9:229–231.

Nadler, M.J., M.C. Hermosura, K. Inabe, A.L. Perraud, Q. Zhu, A.J. Stokes, T. Kurosaki, J.P. Kinet, R. Penner, A.M. Scharenberg, and A. Fleig. 2001. LTRPC7 is a Mg·ATP-regulated divalent cation channel required for cell viability. *Nature.* 411:590–595.

Nelson, N. 1999. Metal ion transporters and homeostasis. *EMBO J.* 18:4361–4371.

Peng, J.B., X.Z. Chen, U.V. Berger, P.M. Vassilev, E.M. Brown, and M.A. Hediger. 2000. A rat kidney-specific calcium transporter in the distal nephron. *J. Biol. Chem.* 275:28186–28194.

Perveen, S., W. Altaf, N. Vohra, M. Bautista, R. Harper, and R. Wapnir. 2002. Effect of gestational age on cord blood plasma copper, zinc, magnesium and albumin. *Early Hum. Dev.* 69:15.

Picard, V., G. Govoni, N. Jabado, and P. Gros. 2000. Nramp 2 (DCT1/DMT1) expressed at the plasma membrane transports iron and other divalent cations into a calcein-accessible cytoplasmic pool. *J. Biol. Chem.* 275:35738–35745.

Romani, A.M., and A. Scarpa. 2000. Regulation of cellular magnesium. *Front. Biosci.* 5:D720–D734.

Runnels, L.W., L. Yue, and D.E. Clapham. 2001. TRP-PLIK, a bifunctional protein with kinase and ion channel activities. *Science.* 291:1043–1047.

Shibuya, I., and W.W. Douglas. 1992. Calcium channels in rat melanotrophs are permeable to manganese, cobalt, cadmium, and lanthanum, but not to nickel: evidence provided by fluorescence changes in fura-2-loaded cells. *Endocrinology.* 131:1936–1941.

Shuttleworth, T.J., and J.L. Thompson. 1996. Evidence for a noncapacitative Ca^{2+} entry during $[Ca^{2+}]i$ oscillations. *Biochem. J.* 316:819–824.

Shuttleworth, T.J., and J.L. Thompson. 1999. Discriminating between capacitative and arachidonate-activated Ca^{2+} entry pathways in HEK293 cells. *J. Biol. Chem.* 274:31174–31178.

Volpe, P., and L. Vezu. 1993. Intracellular magnesium and inositol 1,4,5-trisphosphate receptor: molecular mechanisms of interaction, physiology and pharmacology. *Magnes. Res.* 6:267–274.

Weiss, J.H., and S.L. Sensi. 2000. Ca^{2+}-Zn^{2+} permeable AMPA or kainate receptors: possible key factors in selective neurodegeneration. *Trends Neurosci.* 23:365–371.

Weiss, J.H., S.L. Sensi, and J.Y. Koh. 2000. Zn^{2+}: a novel ionic mediator of neural injury in brain disease. *Trends Pharmacol. Sci.* 21: 395–401.